

Benchmarks in Computational Plasma Physics

P. Londrillo – INAF, Bologna, Italie

S. Landi – Università di Firenze, Italie

What you compute when you do computations of the Vlasov equation?

Overview

- A short review of recent developpements in the numerical integration of the Vlasov equation
- Implementation of high order compact schemes in phase space using upwind methodology, and of multistep Runge-Kutta integrators in time.
- Test of the capability of this approach in classical benchmark problems.
- Are there perspectives to integrate Vlasov equation realistically in multidimensional cases?

Basic

Collisionless plasma can be described following two main models:

- 1 Using a Lagrangian representation whereby a set of $N \rightarrow \infty$ point charges $[x(t), v(t)]$ move under the mean (collective) EM field. The collisionless character of the system is expressed by the conservation of the phase space density (DF) along the particle orbits:

$$f(\mathbf{x}_i(t), \mathbf{v}_i(t)) = f(\mathbf{x}_i(0), \mathbf{v}_i(0)) = C_i$$

- 2 By expressing the DF conservation property as differential equation in the infinite-dimensional phase space

$$D[f] \equiv \left[\frac{\partial}{\partial t} + \mathbf{v} \cdot \nabla_x + \mathbf{F} \cdot \nabla_v \right] f(\mathbf{x}, \mathbf{v}, t) = 0$$

In both representations the Maxwell equations are formulated on an Eulerian framework. Therefore, to evaluate the source terms

$$\rho(\mathbf{x}, t) = \int d\mathbf{v} f(\mathbf{x}, \mathbf{v}, t)$$

$$\mathbf{J}(\mathbf{x}, t) = \int d\mathbf{v} [\mathbf{v} f(\mathbf{x}, \mathbf{v}, t)]$$

also the DF function $f(\mathbf{x}, \mathbf{v})$ need to be represented as an Eulerian field. In the particle method, the link is provided by the Klimontovitch (singular) representation:

$$f(\mathbf{x}, \mathbf{v}, t) = \lim_{N \rightarrow \infty} \frac{1}{N} \sum_i \delta(\mathbf{x} - \mathbf{x}_i(t)) \delta(\mathbf{v} - \mathbf{v}_i(t))$$

Integration schemes in PIC method

The two basic approaches historically follow quite different routes in computational experiences (almost never met).

The PIC implementation method has been formulated and developed more than 20 years ago and then 'frozen' up to now. It is based on the main computational steps:

- (i) Choose a sufficiently high number of macro-particles N_p to sample the true $N \gg N_p$ number of physical particles;
- (ii) Replace delta distribution by some smoother shaping function allowing to assign point charges to a grid (to compute density and currents) and to interpolate field data on each particle;

$$\delta(\mathbf{x} - \mathbf{x}_i(t)) \delta(\mathbf{v} - \mathbf{v}_i(t)) \rightarrow S(\mathbf{x} - \mathbf{x}_i) S(\mathbf{v} - \mathbf{v}_i) \quad \int d\mathbf{x} d\mathbf{v} S(\mathbf{x} - \mathbf{x}_i) S(\mathbf{v} - \mathbf{v}_i) = 1$$

- (iii) Integrate particles orbits in time by the (2-th order, centered) Leap-frog scheme;
- (iv) Integrate the Maxwell equations for the (**E,B**) fields by an equivalent leap-frog scheme (now in space and time), usually referred to as Yee's module.

Integration schemes in Vlasov equation

In recent years, the numerical experience on grid-based Vlasov equation enjoyed a growing interest and development. Several papers testing and comparing different codes have been produced (some are considered below).

When reducing the Vlasov differential equation from infinite to a finite N-dimensional space, we perform implicitly some kind of coarse-graining, typically a cell average or truncation in Fourier space, replacing f with $\langle f \rangle$. We get then a new exact equation:

$$\hat{D}[\langle f \rangle] = -\nabla_x \cdot \langle \delta \mathbf{v} \delta f \rangle - \nabla_v \cdot \langle \delta \mathbf{F} \delta f \rangle$$

where $\delta f = f - \langle f \rangle$ and so on.

The rhs terms represent cell-averaged contributions of small unresolved scales.

We are then faced with a problem of closure akin to the fluid turbulence case, but now much more difficult, because we do not know how small scales may affect the large scale structures. In particular modelling the free-streaming effect on the unresolved velocity small scales (the first one on the rhs) is a classical open problem.

When solving the Vlasov equation by some numerical scheme, we replace the unknown rhs term by a numerical Truncation Error (TE).

Stable integrators entail a TE which has a dominant (asymptotic) diffusive behavior, with size depending on the scheme order. As consequence:

1- Among all possible physical regimes of a collisionless plasma, a Vlasov code correctly represents only those where unresolved physics can be neglected or, otherwise, where it has a dominant diffusive behavior

2 – Basic plasma phenomena, like wave-particles interactions, Landau damping, formation of coherent structures, and so on, which cannot be modelled by collisional-like behaviors, need to be resolved explicitly

In either cases, schemes with small numerical diffusivity have to be preferred, to assure a maximum of resolution. Since available grid sizes are quite limited in multidimensional problems, only high-order integrators in space and time can provide the 'optimal' resolution with 'reasonable' numbers of grid points.

Existing Vlasov codes are based on low-order integrators, the basic building-block being the so called 'splitting scheme' (analogous to the leap-frog-Yee module in PIC).

The main reason for this choice relies on the assumption that spectral (or spectral-like) integrators are unstable, and must be corrected or limited (using some filtering).

We will show this is not true, if space-time integrators are properly chosen, in a way to take into account the underlined mathematical structure of the Vlasov equation. Infact:

1- The Vlasov equation is hyperbolic and upwind derivatives provide stable algorithms while central differentiation schemes (finite differences or spectral) may give instead oscillatory behaviors. The main reason is that upwinding entails a small diffusivity, damping the highest frequencies.

2 – The size of TE depends not only on the scheme formal order but also on the regularity of the solution in phase-space. Numerical analysis of the Vlasov equation assures the existence of regular (differentiable) solutions in time. This allows to estimate the TE

$$TE = C (h k_{eff})^r f^{(1)}$$

where C is a numerical constant decreasing as the order r increases.

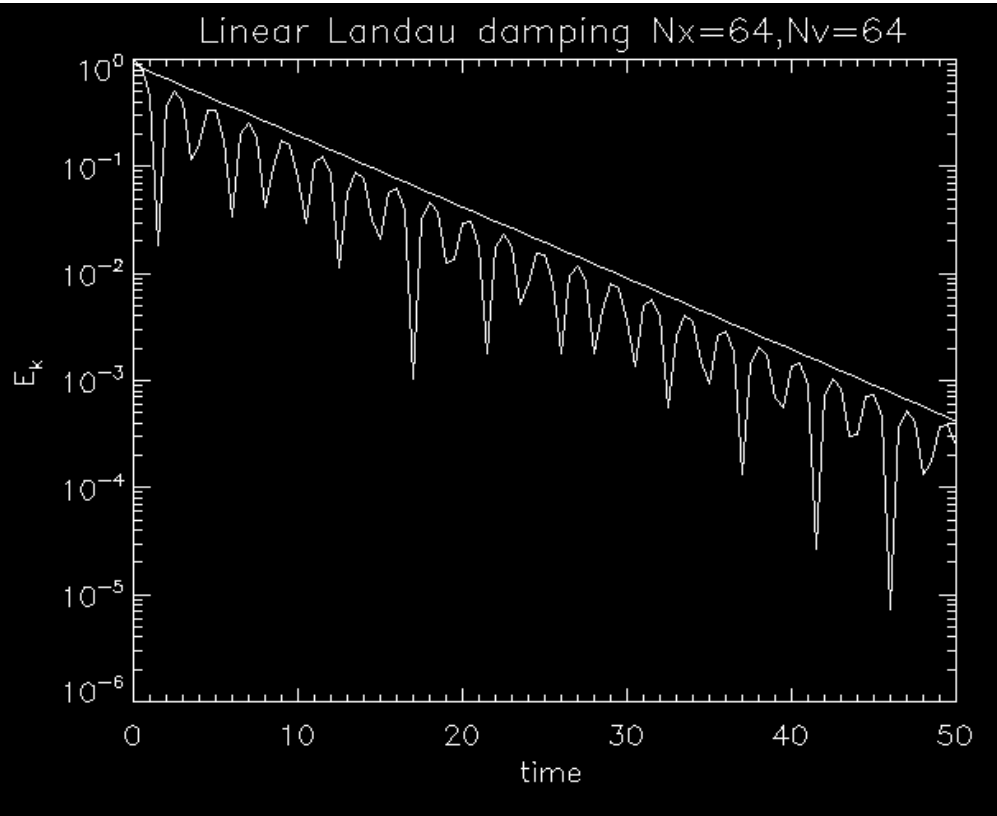
Testing a new high-order compact upwind scheme.

We present preliminary results on some classical benchmark problems for 1D electrostatic cases (Arber & Vann, 2002; Filbet & Sonnendrucker, 2003; Califano et al., 2006)

The code is based on the following recipes:

- 1) Derivatives in (x,v) coordinates are performed using upwind 5th or 7th order compact algorithms.
- 2) Upwinding in the x -derivative is defined by the (positive or negative) sign of the v -coordinate.
- 3) Upwinding in the v -derivative is defined by the sign of the $F(x,t)$ field (the acceleration characteristic)
- 4) For integration in time, time-splitting is replaced by 3th or 4th order Runge-Kutta scheme.
- 5) Electric field can be obtained either using Poisson equation or Ampere law.

1 – Linear Landau damping



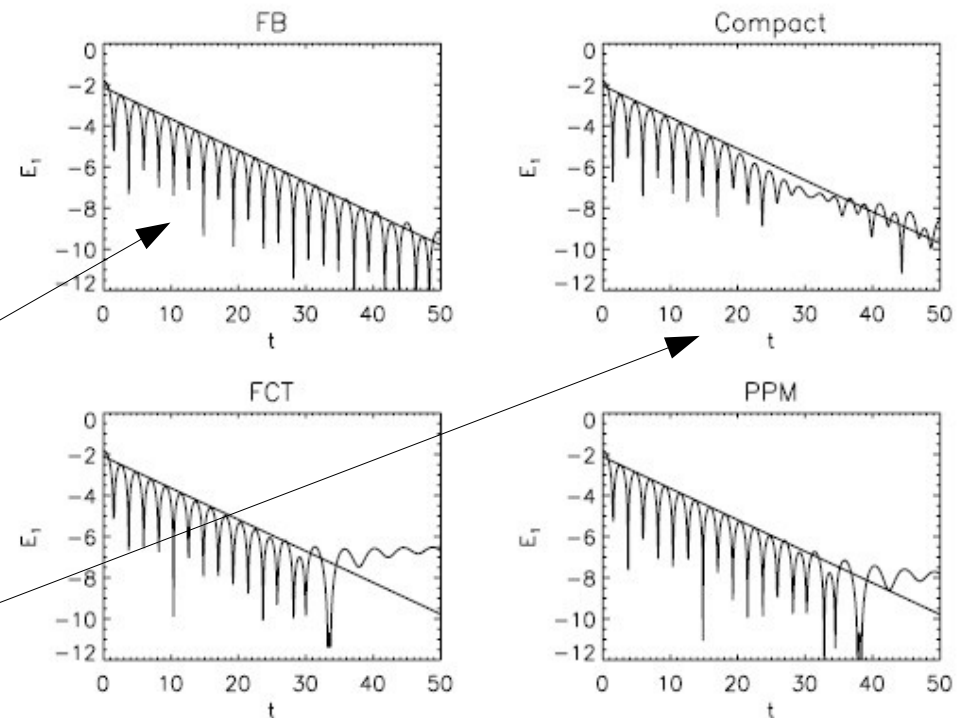
Our code:

correct value of the damping rate

accurate averaged decay rate also at late time (before recurrency time however)

Same accuracy of Flux Balanced (FB) schemes

Upwind compact schemes avoid problems with compact centered algorithm with filters.

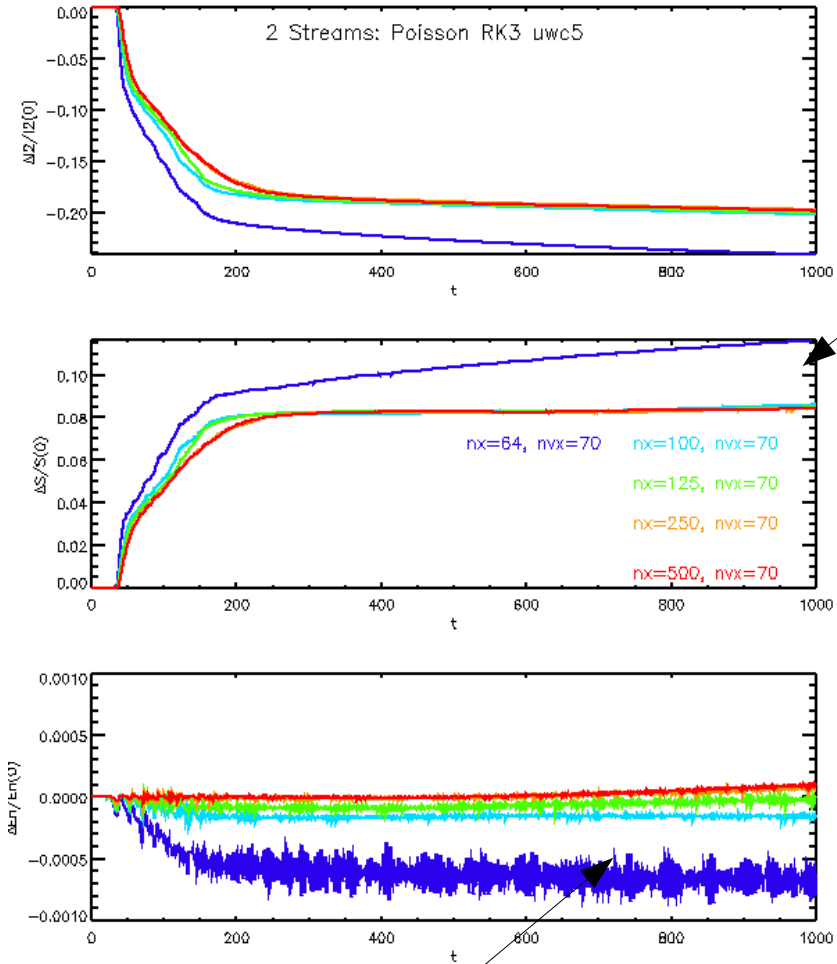


Linear Landau damping test for different algorithms (Arber & vann, 2002)

2 – Two stream instability

$$L_x = 100 \quad v_e^{max} = 7$$

Entropy variations within 8%



Energy conservation accurate within 0.01%

Convergence achieved at nx=100

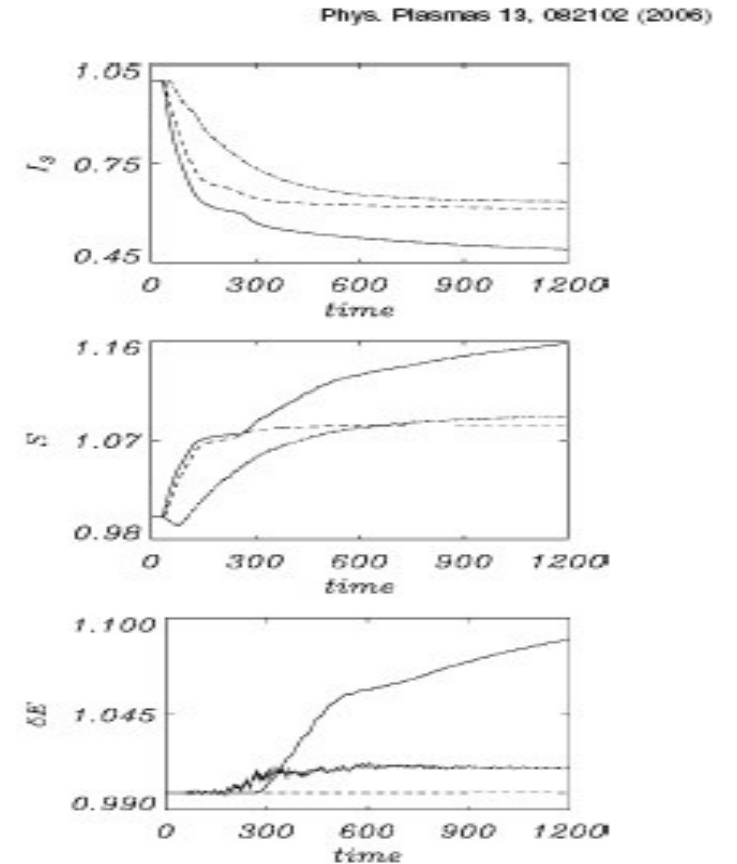
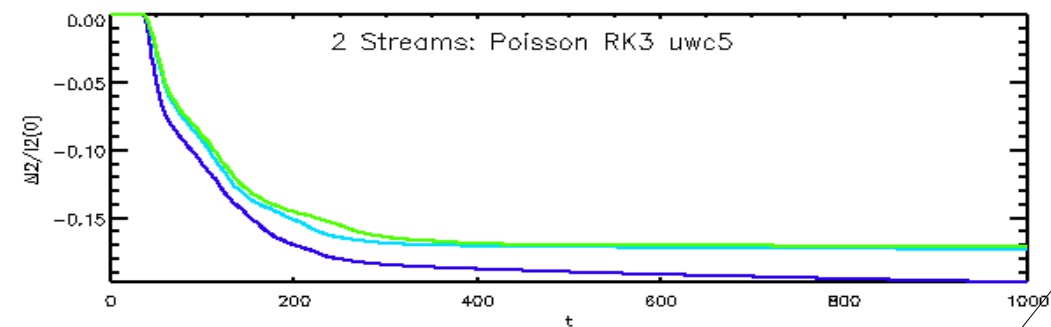
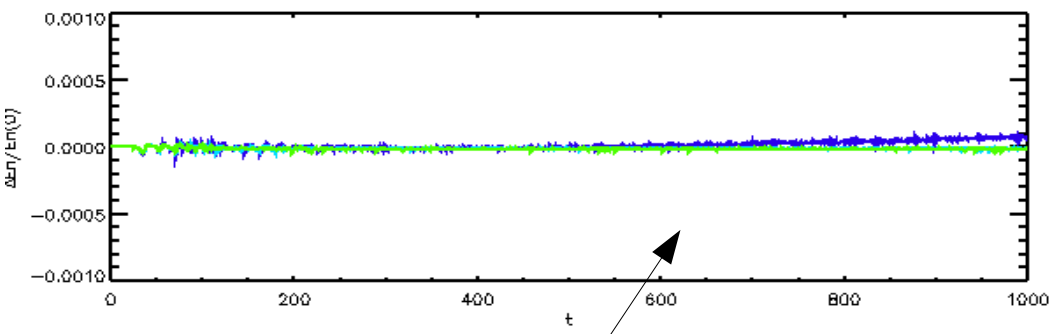
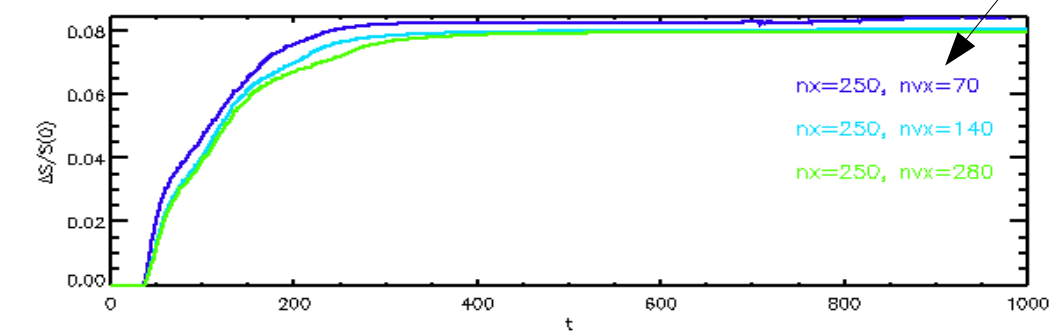


FIG. 2. (a)–(c) The time evolution of the third order invariant I_3 , of the entropy S and of the energy fluctuations δE , first, second, and third frame, respectively. Continuous, dashed, and point-dashed lines correspond to VL2, VL3, and SPL run, respectively.

Same two stream instability test using VL2, VL3 and SPL methods and resolution $N_x=1000$, $N_v=140$ (Califano et al., 2006)



Entropy variations within 8%



Energy conservation accurate within 0.01%

Convergence achieved at $N_v=70-140$

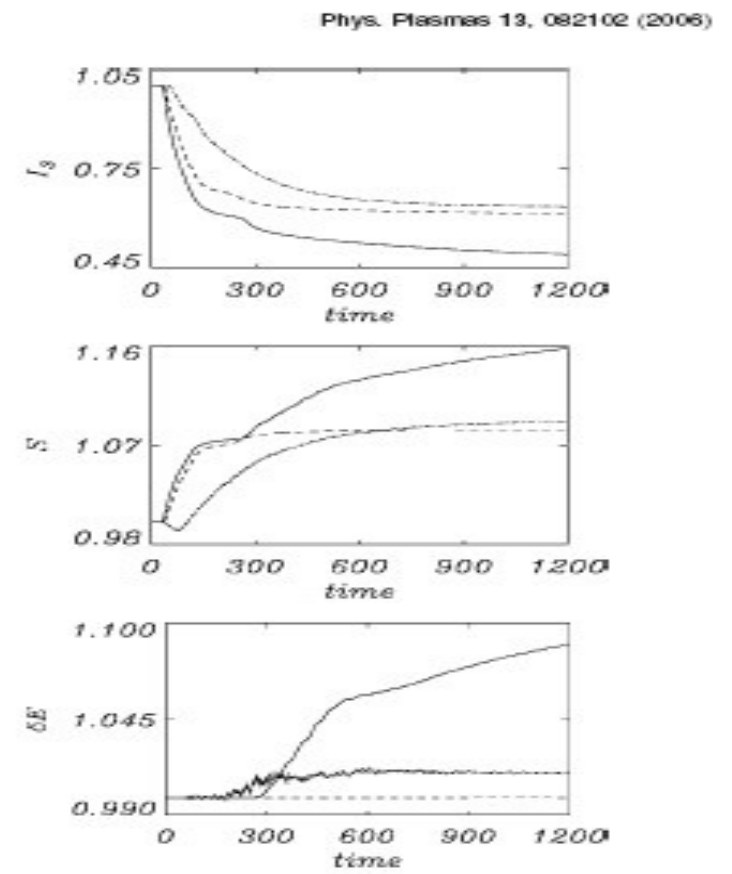
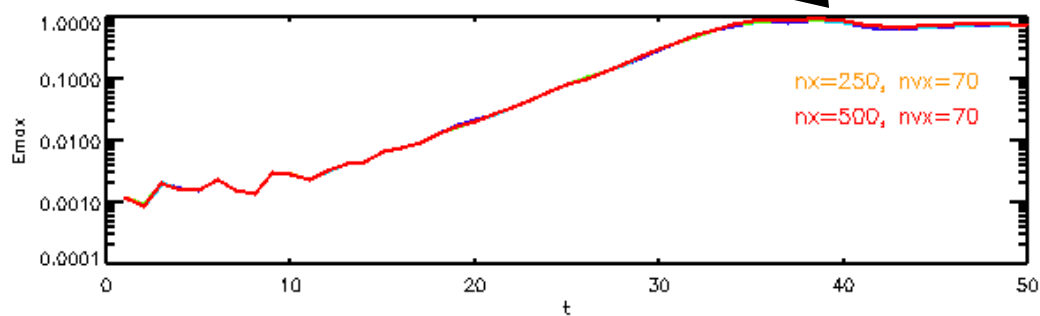
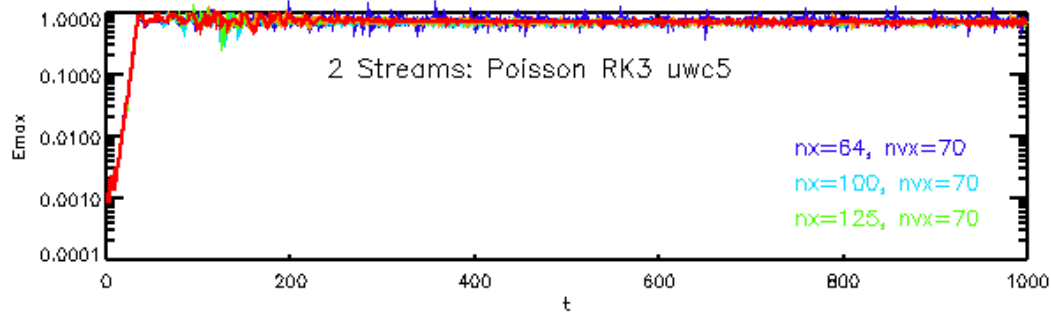


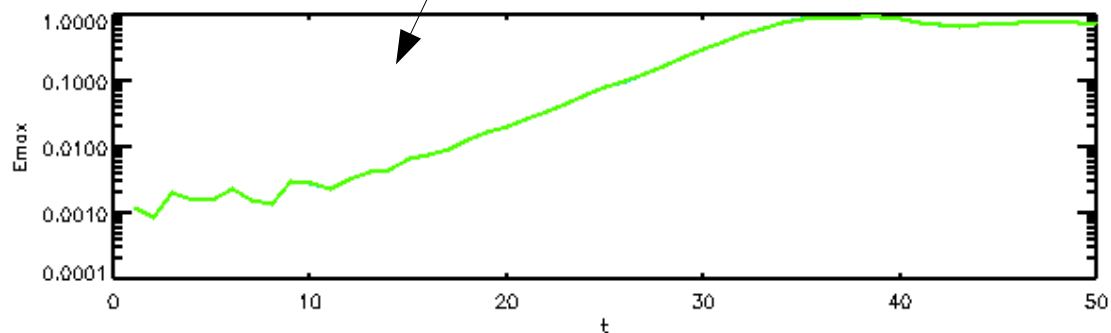
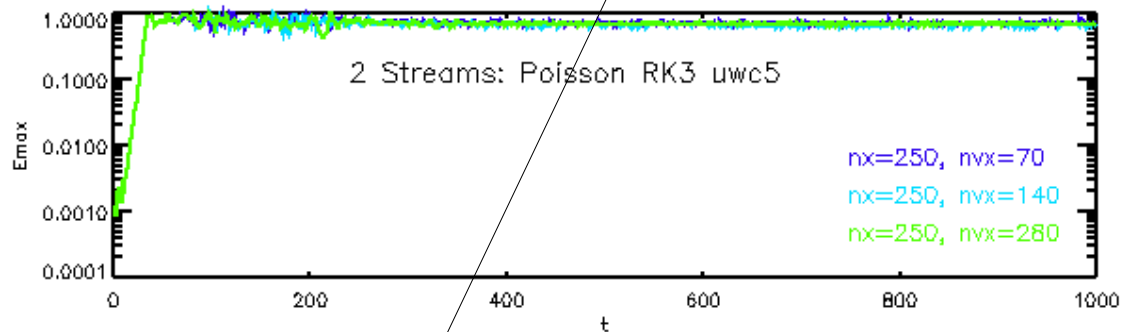
FIG. 2. (a)–(c) The time evolution of the third order invariant I_3 , of the entropy S and of the energy fluctuations δE , first, second, and third frame, respectively. Continuous, dashed, and point-dashed lines correspond to VL2, VL3, and SPL run, respectively.

Same two stream instability test using VL2, VL3 and SPL methods and resolution $N_x=1000$, $N_v=70$ (Califano et al., 2006)

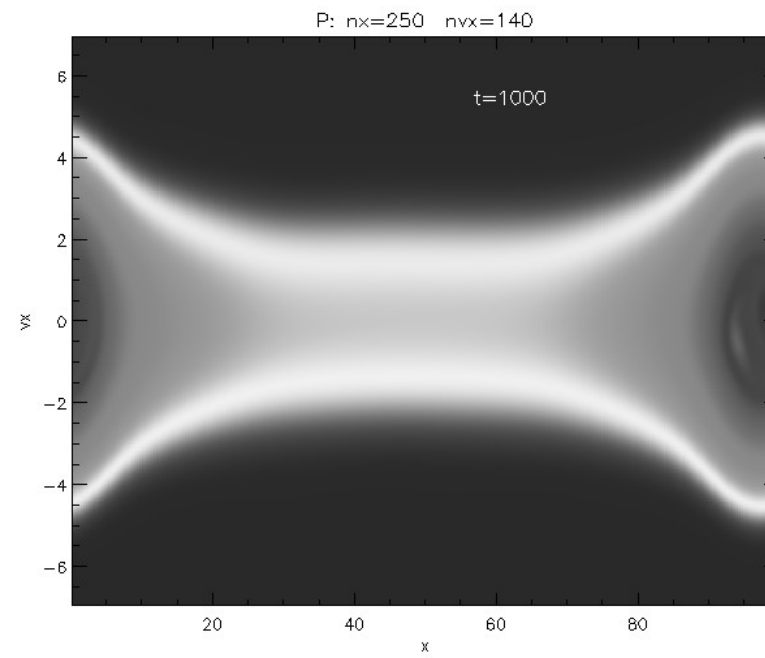
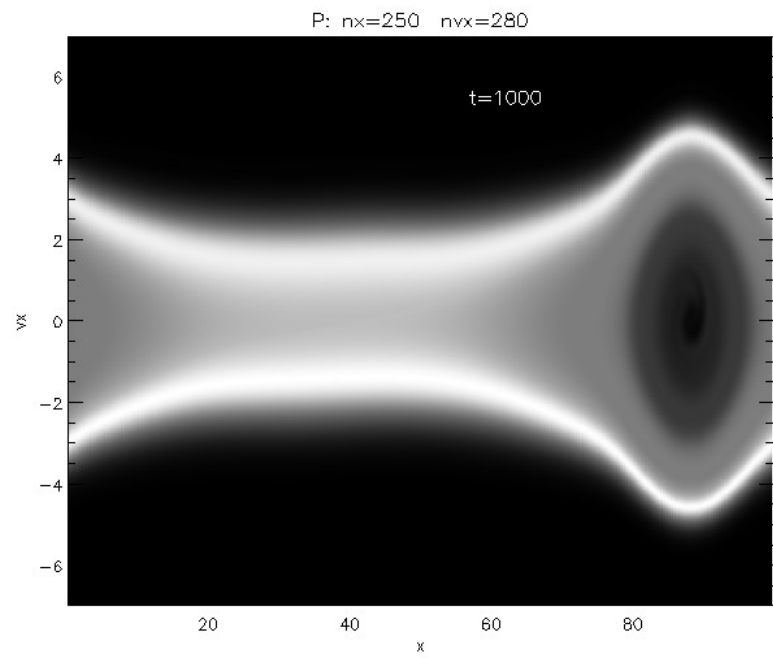
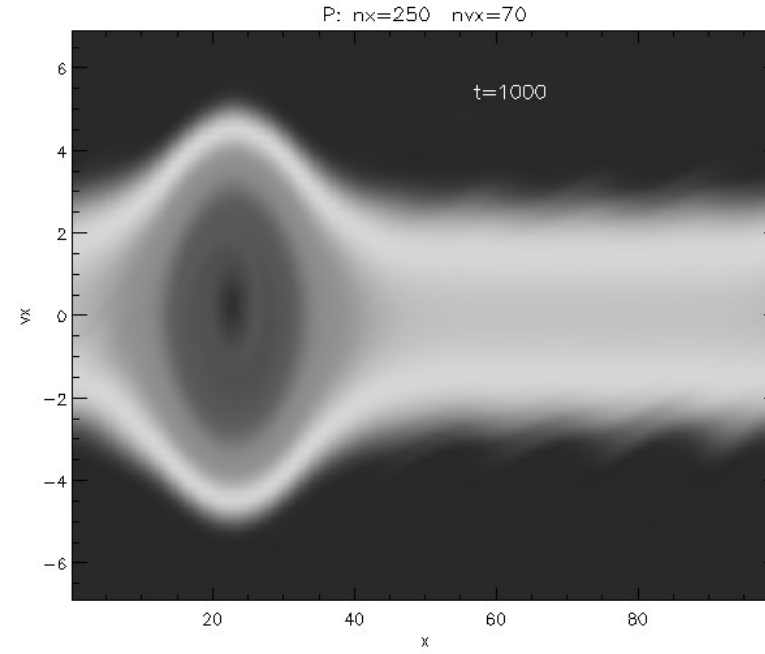
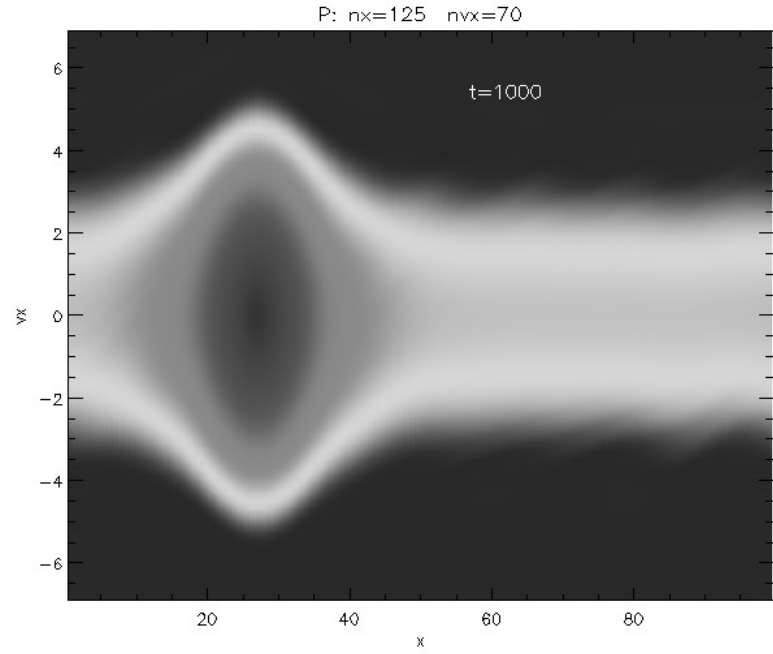


Linear growth rate well reproduced independently of the adopted resolution both in N_x and N_v

Electrostatic energy as function of time for different N_x .
Up: whole simulation; down: first 50 times



Electrostatic energy as function of time for different N_v .
Up: whole simulation; down: first 50 times



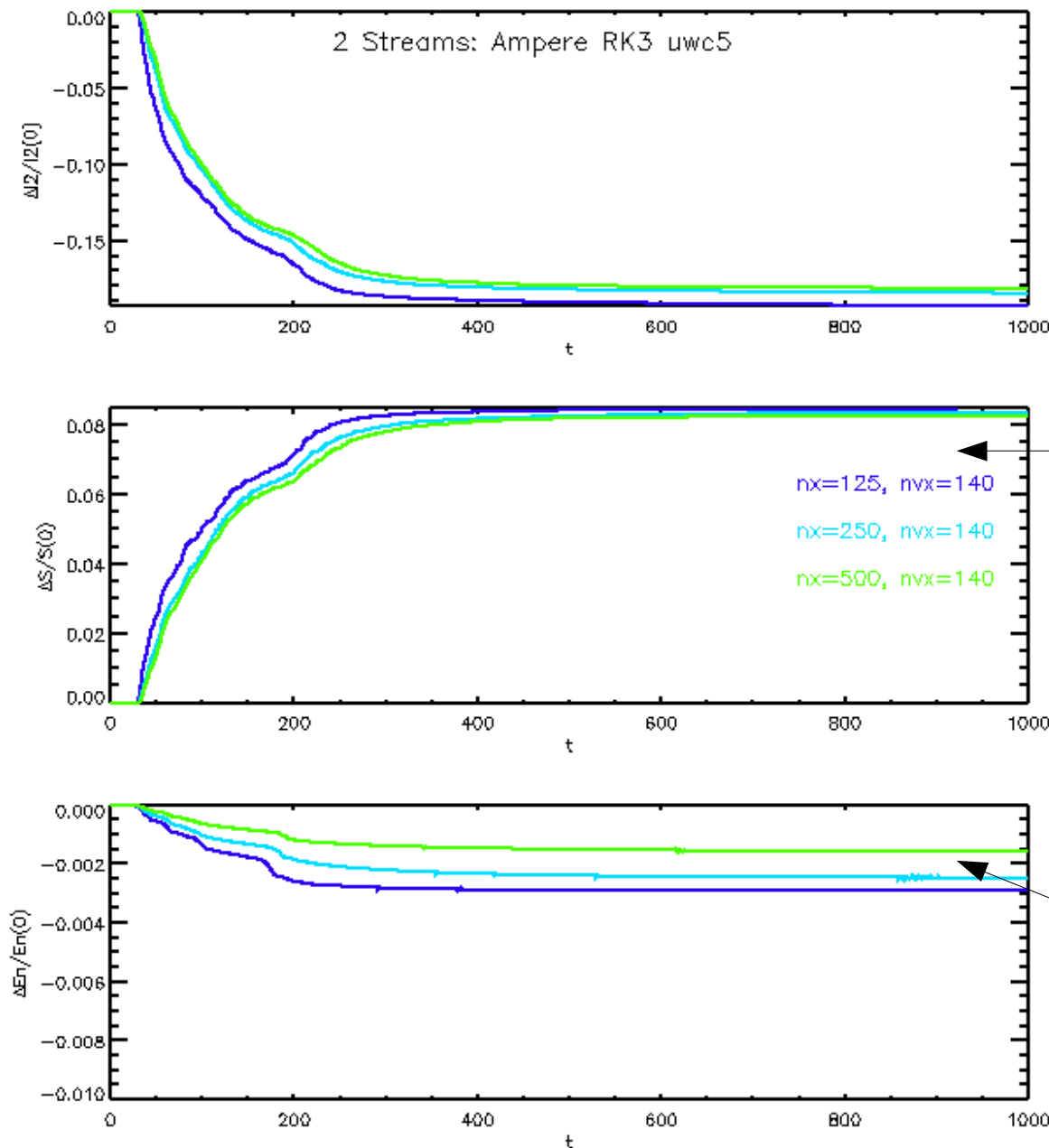
The DF in phase space at $t=1000$ for different resolutions

2 – Two stream instability

Poisson replaced by Ampere

Entropy variations are not affected by the use of Ampere law instead of Poisson equation.

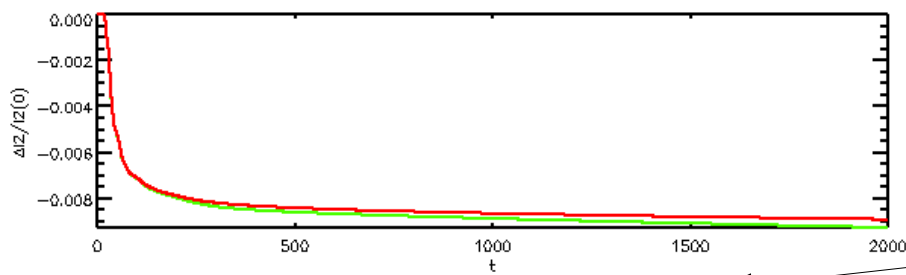
Energy conservation is significantly affected by time integration of the Ampere law (however energy is conserved within less than 1% !).



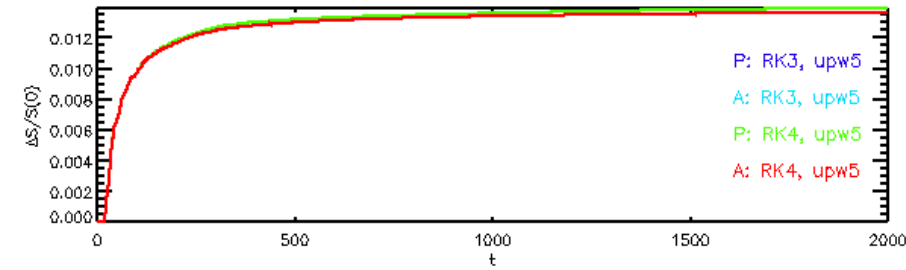
Two stream instability test using the Ampere law instead of the Poisson equation for the electric field.

3 - Bump on Tail

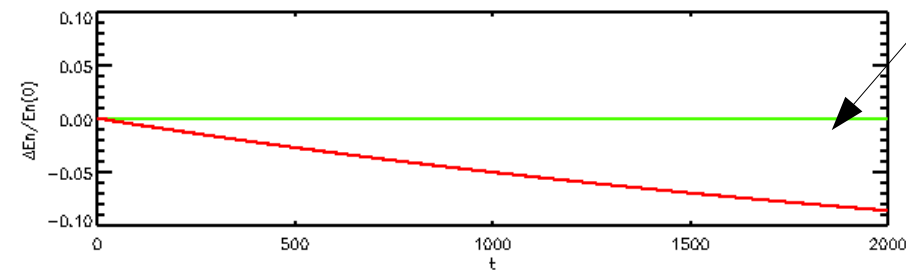
$$L_x = \frac{2\pi}{0.3} \quad v_e^{max} = 8$$



Entropy variations of 1.2% for all cases



As for the two-streams instability energy is much better conserved using Poisson equation.



Bump on Tail test performed on a 128x128 grid, using both Ampere and Poisson laws and for different integration schemes.

With an high-order Upwind Compact scheme we do NOT observe negative variations of the entropy.

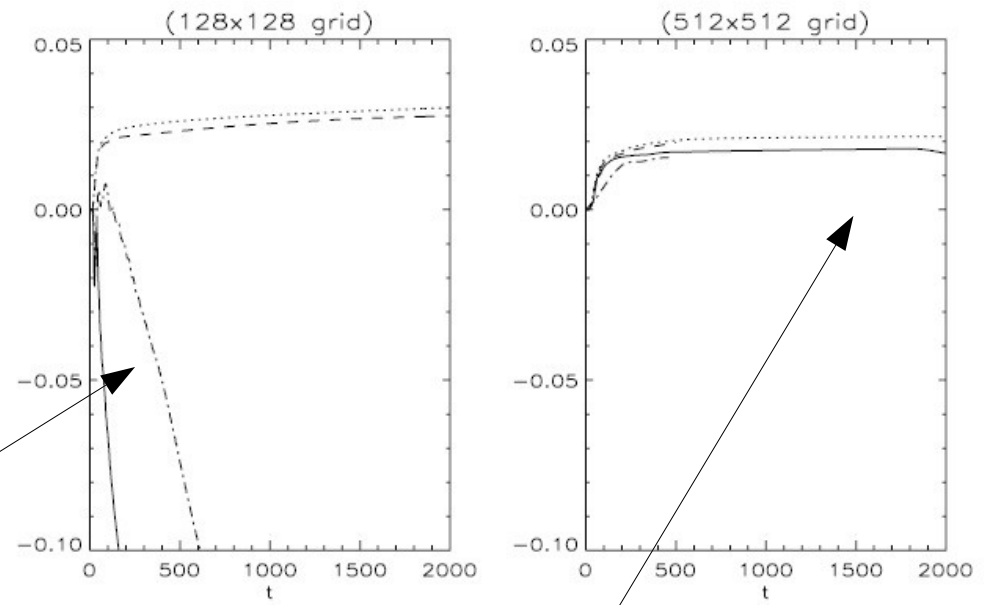


FIG. 4. Time evolution of the fractional change in discrete kinetic entropy for the bump-on-tail test with resolution (128, 128) and (512, 512). The solid line is for FB, the dotted line is PPM, the dashed line is FCT, and the dash-dotted line is Compact.

Entropy conservation is comparable to (even better than) that obtained using a 512x512 grid with FB, PPM, or FCT methods (Arber & Vann, 2002).

3 - Bump on Tail

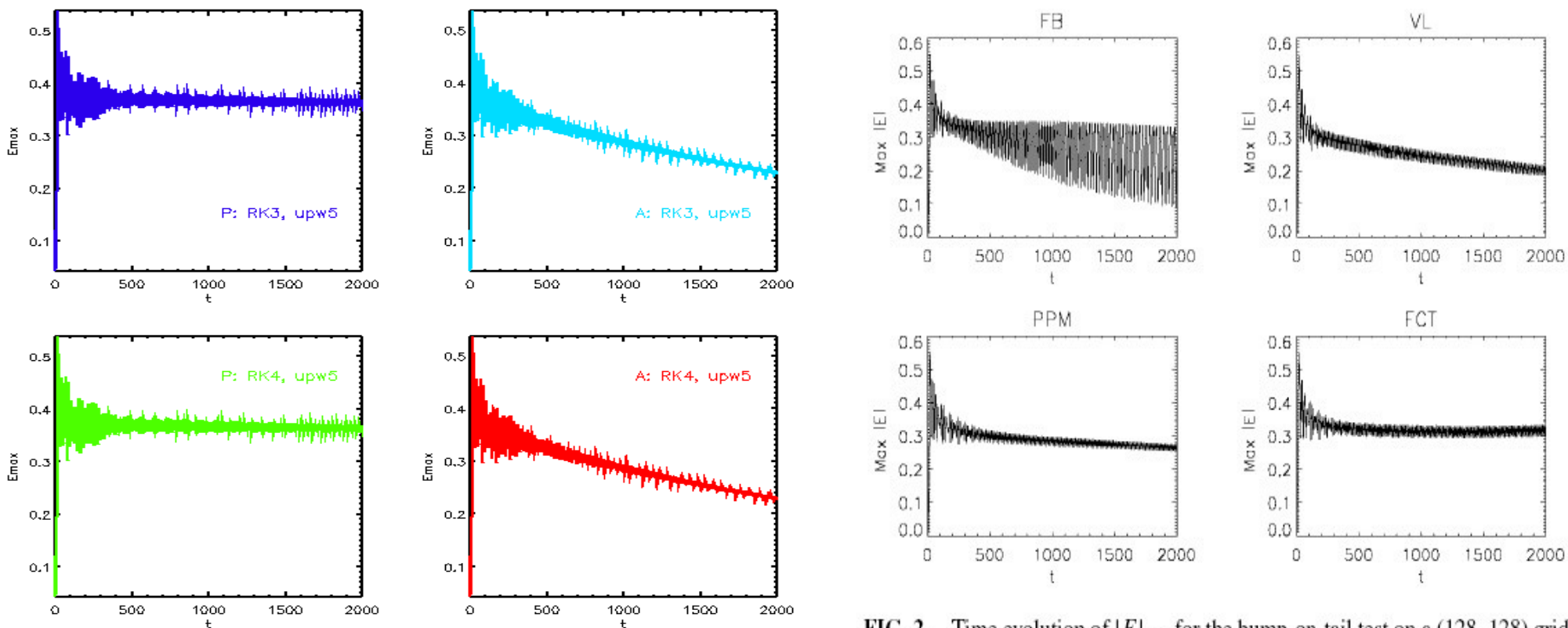
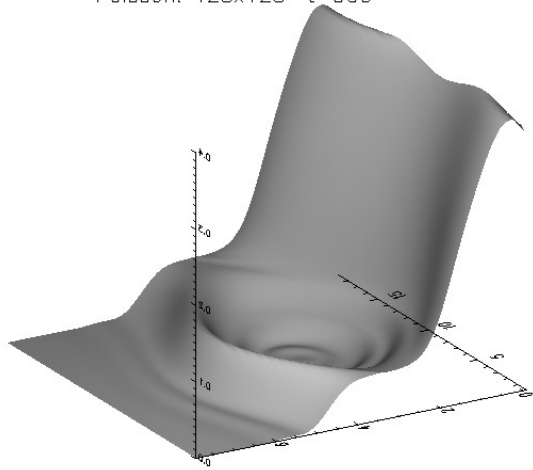


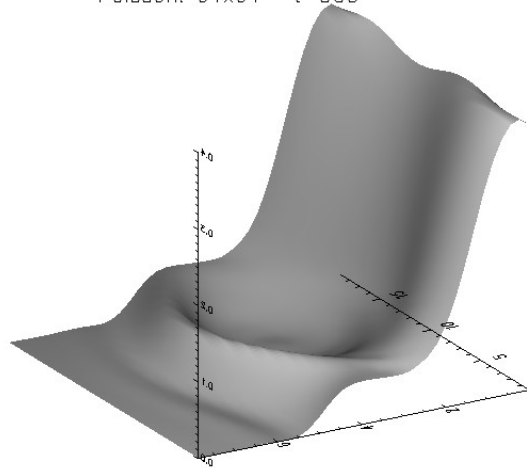
FIG. 2. Time evolution of $|E|_{\max}$ for the bump-on-tail test on a (128, 128) grid.

No large oscillation in the electric field (as seen in FB) nor dissipation of E_{\max} (as observed in low order schemes as VL2) when using Poisson.

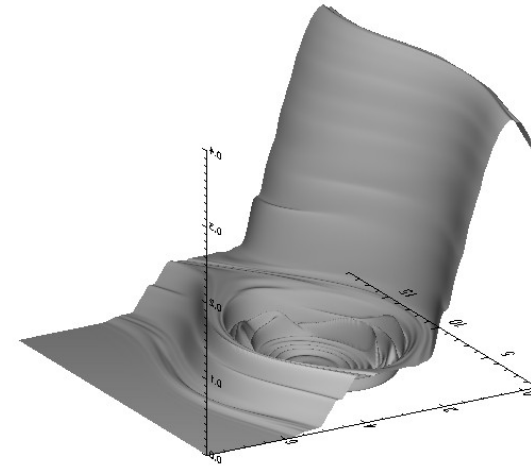
Poisson: 128x128 t=500



Poisson: 64x64 t=500



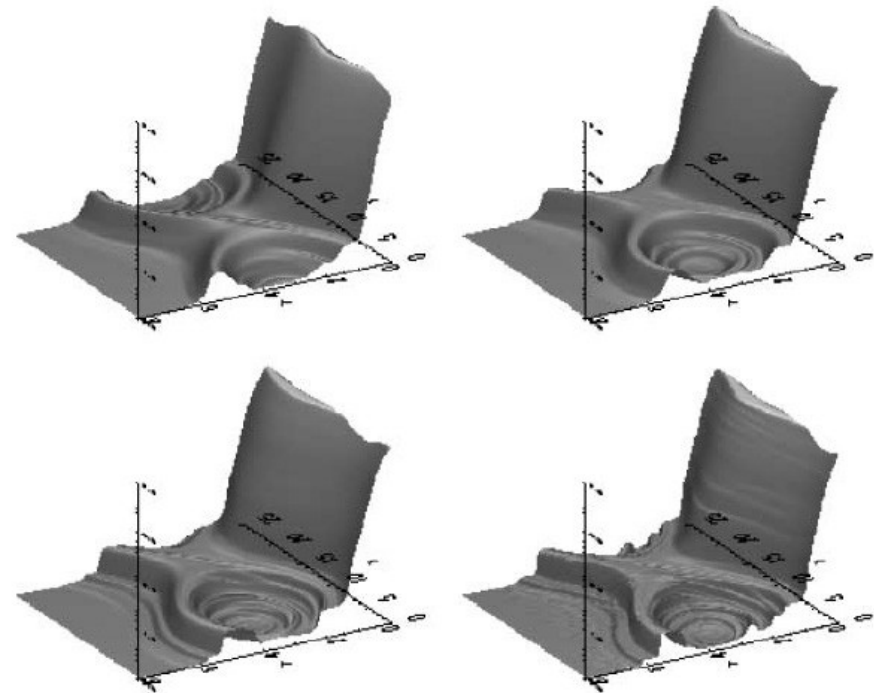
Poisson: 512x512 t=500



Bump-on-tail phase space holes at t=500 with a different grids using a 5-th order upwind compact scheme and a 3-th order RK scheme. Electric field is obtained by using the Poisson equation.

Rather good small scales resolution also with coarser grids.

Smooth solution at higher resolutions without signs of terracing.



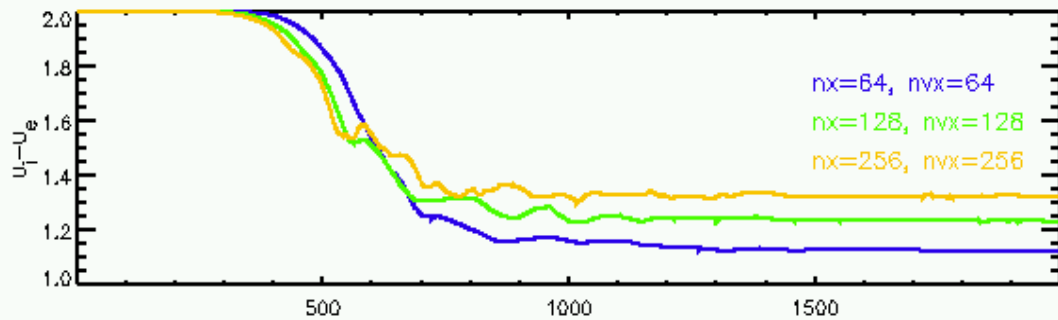
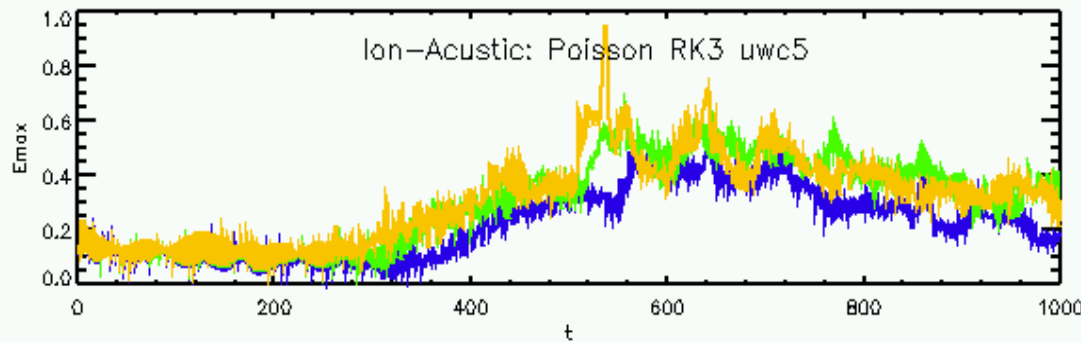
Bump-on-tail phase space holes at t=500 with a 512,512) grid using different schemes: FB (top left), VL (top right), PPM (bottom left) and FCT (bottom right). From Amber & Vann, 2002.

4 – Ion Acoustic wave test

$$L_x = \frac{2\pi}{0.05} \quad v_e^{max} = 8$$

Convergence in the time of the onset of decay

Small differences in the asymptotic value of the drift velocity



Time evolution of $|u_i - u_e|$ for different resolutions using a 5-th order Compact Upwind scheme with a 3-th order RK scheme. Electric field is computed using Poisson.

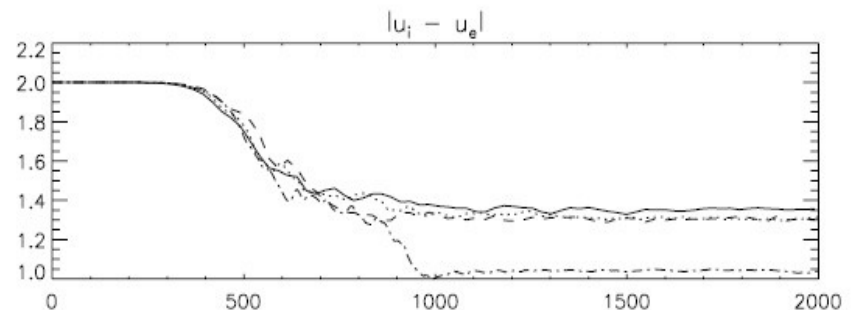
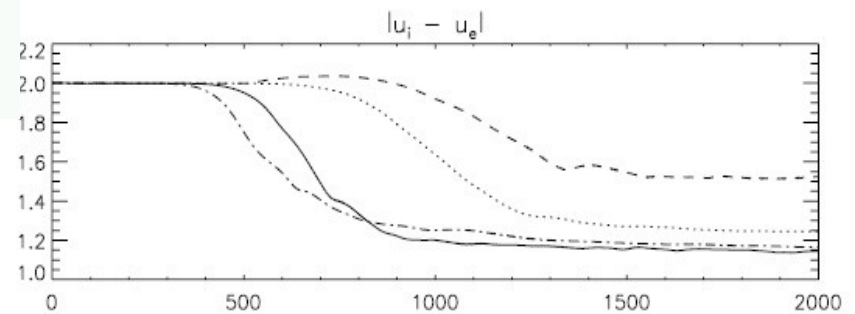
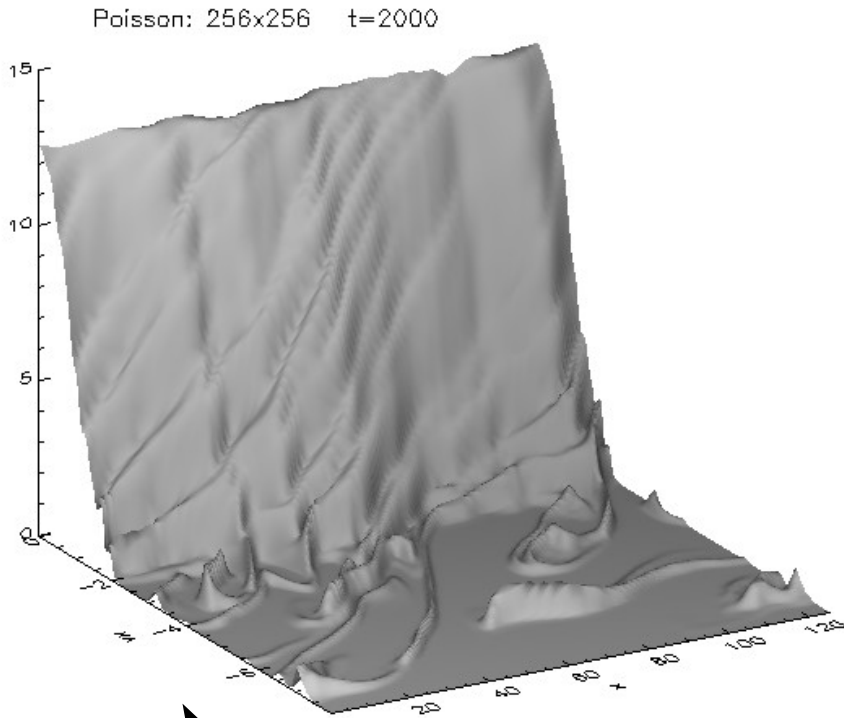


FIG. 8. Evolution of the $|u_i - u_e|$ for the PPM, FB, VL, and FCT schemes on two resolutions. In both plots the solid lines are PPM, the dotted lines are VL, the dashed lines are FB, and the dot-dashed lines are FCT. The upper figure is on a (64, 64) grid and the lower figure is on (512, 512).



Ion DF at $t=2000$ for the Ion acoustic test with a 5-th order upwind compact scheme with 3-th order RK time step scheme. Electric field obtained via Poisson equation.

No terracing or clipping of the ion DF is observed (to be compared to the FCT case)

Smooth profiles for the DF

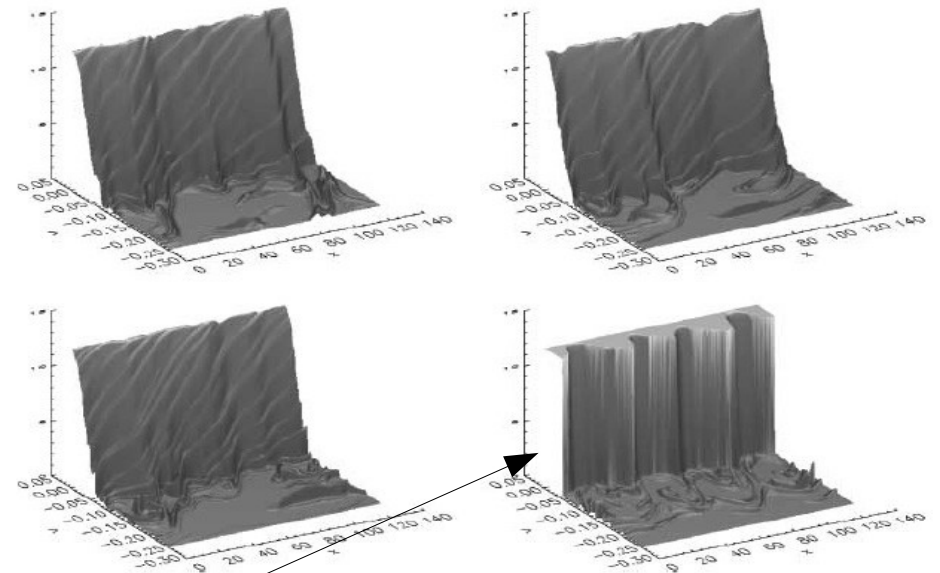


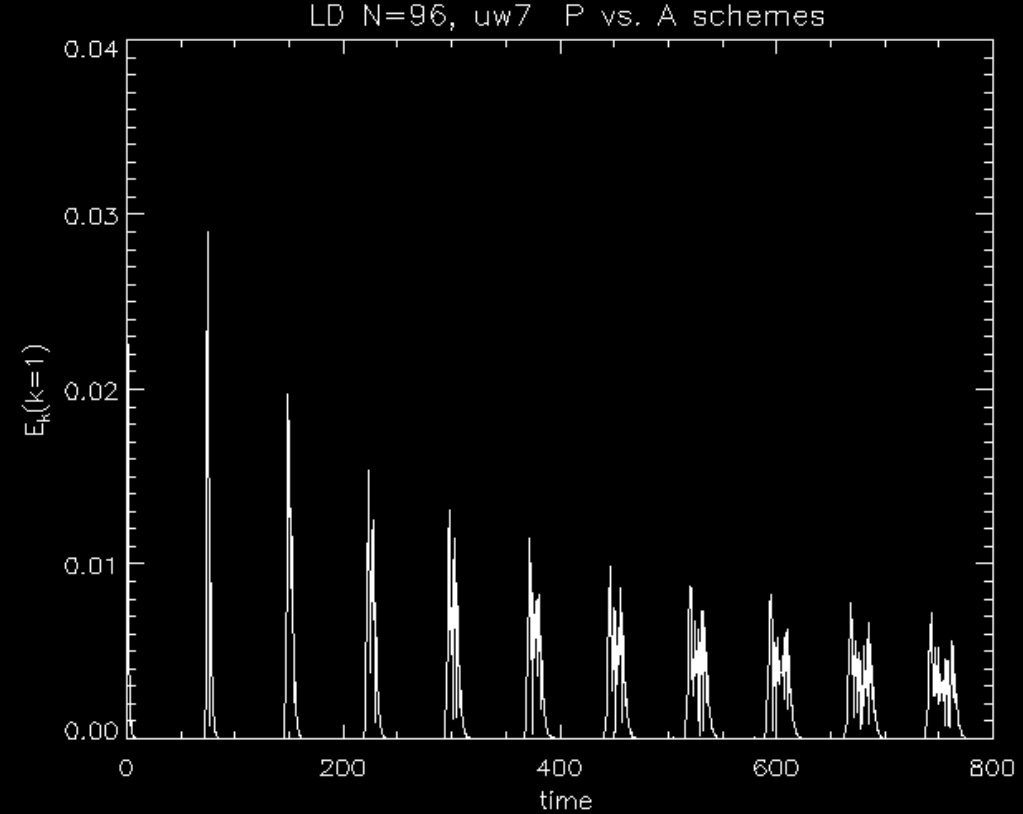
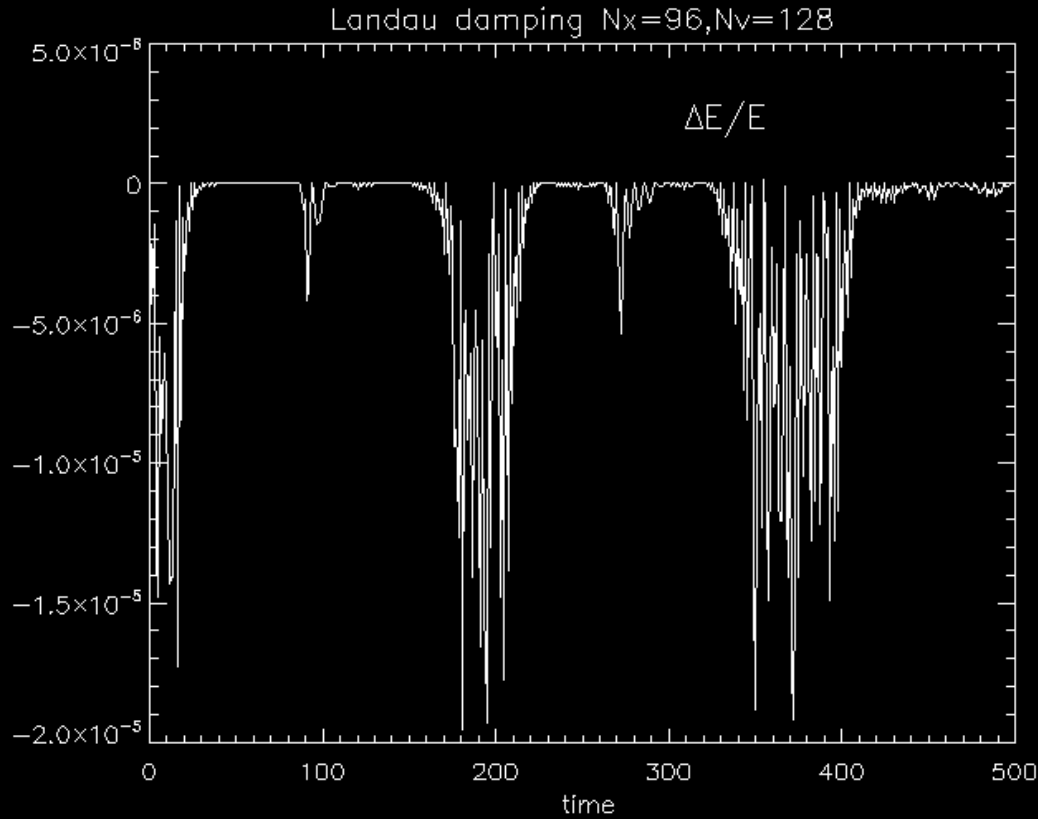
FIG. 9. Ion-acoustic turbulence test at $t = 2000$ with a $(512, 512)$ grid for the FB (top left), VL (top right), PPM (bottom left), and FCT (bottom right) methods. Shown are shaded surfaces of f_i for the whole of x but with only $-8 < v_i < 0$.

Ion DF at $t=2000$ with a $(512,512)$ grid using different schemes (Arber & Vann, 2002)

Non-linear Landau damping in a single-mode wave

- The long-time evolution of the Landau damping problem can be studied only by using a very large number of grid points in phase space.
- In fact, a numerical integration makes sense for time $t < T_R$ (the recurrence time), defined as the time where a finite grid in v -space is no longer sufficient to resolve filamentation.
- Here we show how compact schemes behave in the opposite case $t \gg T_R$

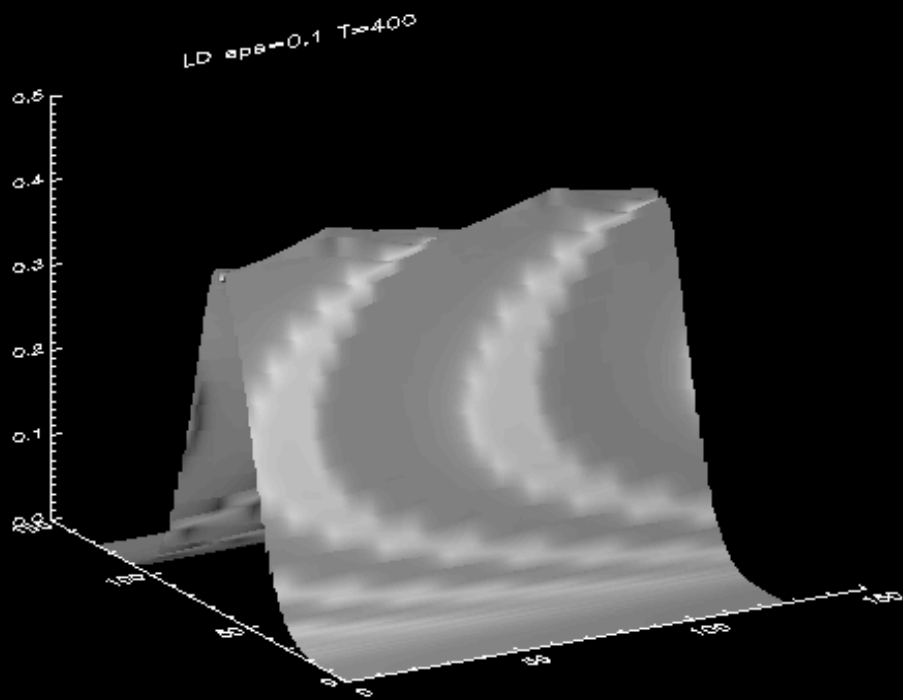
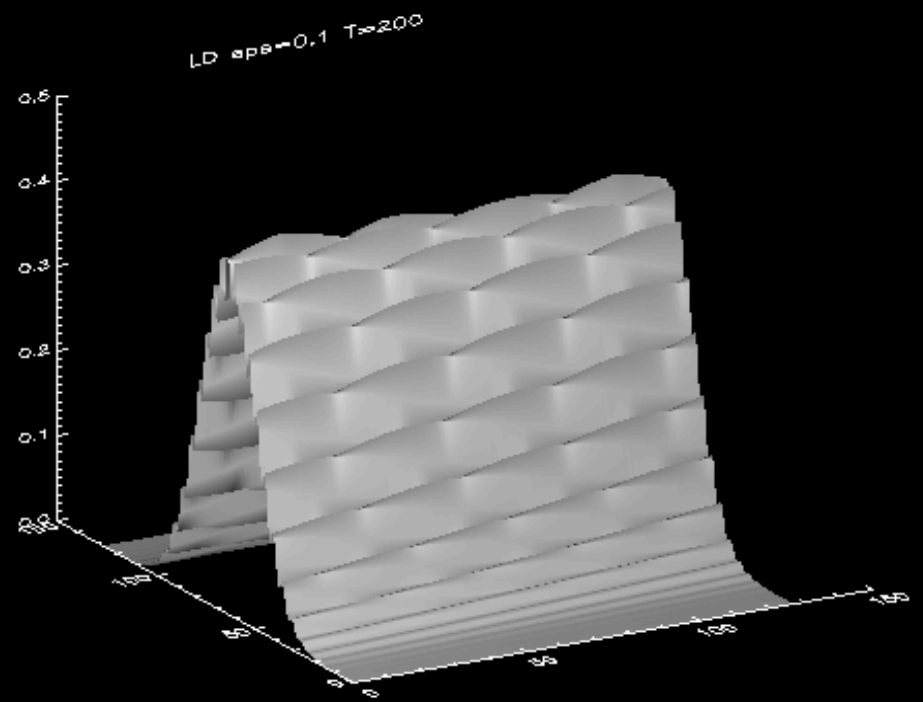
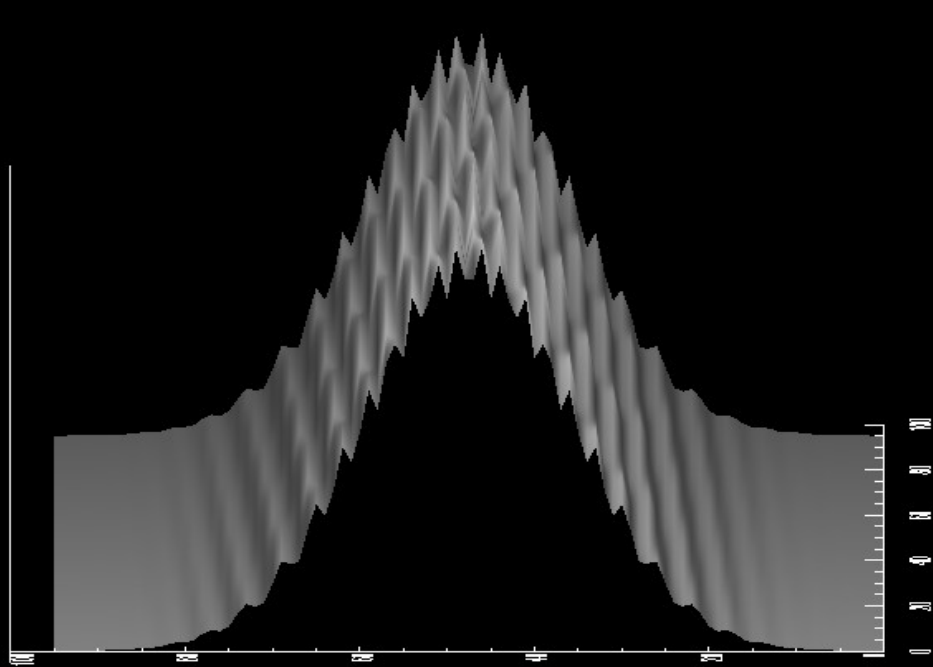
Filamentation: some tests



Total energy variations (left) and electric power (right) in the fundamental mode as function of time for Landau damping simulations. Time evolution of the energy power is shown for simulations using either Poisson and Ampere laws.

Very good energy conservation

Correct recurrency time for both Poisson and Ampere laws



Some example of filamentation in Landau damping tests

Conclusions

- High order spectral-like schemes to compute phase space derivatives and Runge-Kutta integrators in time may assure sufficient resolution with reasonable grid sizes.
- Upwind technique provides a minimum of numerical diffusivity still assuring stability.
- This makes feasible Vlasov computations even in multidimensional electromagnetic case.
- However, low numerical diffusivity makes more evident problems related to filamentation.